



The Discovery and Evolution of a Radio Continuum and Excited-OH Spectral-line Outburst in the Nearby Galaxy NGC 660

Downloaded from: <https://research.chalmers.se>, 2024-12-23 15:28 UTC

Citation for the original published paper (version of record):

Salter, C., Ghosh, T., Minchin, R. et al (2024). The Discovery and Evolution of a Radio Continuum and Excited-OH Spectral-line Outburst in the Nearby Galaxy NGC 660. *Astronomical Journal*, 168(6).
<http://dx.doi.org/10.3847/1538-3881/ad812d>

N.B. When citing this work, cite the original published paper.



The Discovery and Evolution of a Radio Continuum and Excited-OH Spectral-line Outburst in the Nearby Galaxy NGC 660

C. J. Salter¹, T. Ghosh², R. F. Minchin³ , E. Momjian³ , B. Catinella⁴ , M. Lebron⁵, and M. S. Lerner⁶

¹Retired, Arecibo Observatory, HC3 Box 53995, Arecibo, PR 00612, USA; csalter.wfc@gmail.com

²Retired, Green Bank Observatory, P.O. Box 2, Green Bank, WV 24944, USA; tapasig91@gmail.com

³National Radio Astronomy Observatory, 1003 Lopezville Road, P.O. Box O, Socorro, NM 87801, USA; rminchin@nrao.edu, emomjian@nrao.edu

⁴ICRAR, The University of Western Australia, 35 Stirling Highway, Crawley, WA 6009, Australia; barbara.catinella@uwa.edu.au

⁵University of Puerto Rico, P.O. Box 23323, San Juan, PR 00931-3323, USA; mayra.lebron3@upr.edu

⁶Department of Space, Earth and Environment, Chalmers University of Technology, Onsala Space Observatory, SE-43992 Onsala, Sweden; mikael.lerner@chalmers.se

Received 2023 July 23; revised 2024 September 10; accepted 2024 September 26; published 2024 November 13

Abstract

Arecibo 305 m Telescope observations between 2008 and 2018 detected a radio continuum and spectral-line outburst in the nearby galaxy, NGC 660. Excited-OH maser emission/absorption lines near 4.7 GHz, and H₂CO absorption at 4.83 GHz varied on timescales of months. Simultaneously, a continuum outburst occurred in which a new compact component appeared, with a GHz-peaked spectrum and a 5 GHz flux density that rose to a peak value of about 500 mJy from 2008.0 to 2012.0. Follow-up interferometric continuum images from the Very Large Array at 10 GHz of this new continuum component determined it to be located at the nucleus of NGC 660. Subsequent High Sensitivity Array line and continuum very long baseline interferometry observations of the NGC 660 nucleus revealed a morphology that appears to be consistent with rapidly precessing, mildly relativistic jets from the central black hole. While requiring detailed modeling, this strongly suggests that the outburst is due to nuclear activity. From its timescale, the shape of the continuum light curve, and the milliarcsec radio structure, the most likely cause of the outburst is active galactic nuclei-type activity of accretion of a gas cloud onto the central black hole.

Unified Astronomy Thesaurus concepts: [Galaxies \(573\)](#)

1. Introduction

At a redshift of $z = 0.003$, the “peculiar” galaxy NGC 660 has highly unusual properties. While classified as type SBa, its gas-rich inner disk has a composite LINER/H II spectrum, and its far infrared luminosity of $\log(L_{\text{FIR}}) = 10.3$, makes it a luminous infrared galaxy (LIRG). In addition, it possesses a component that is strongly warped out of the plane of the main disk, and an outer quasipolar ring. NGC 660 also shows strong ($S_{1.4 \text{ GHz}} = 373 \text{ mJy}$) radio-continuum emission of size about $32'' \times 15''$, and a more compact central double/edge-on component of size $\sim 4''$. With 210 mas resolution, M. E. Filho et al. (2002) claimed to have located a compact core of 8.4 GHz flux density $\sim 3 \text{ mJy}$. The radio continuum spectrum in the centimeter range is that expected from synchrotron emission (see the solid black line in Figure 3).

In 2008, the current authors detected a surprisingly rich cm wavelength (1.1–10 GHz) molecular-line spectrum from the prototypical ultraluminous infrared galaxy, Arp 220 (C. J. Salter et al. 2008). This included the presence of such species as the “prebiotic molecule” CH₂NH, CH and H₂CO in emission, with transitions of HCN ($v_2 = 1$) and excited OH, plus probably CH₃OH, in absorption. This was then followed up with Arecibo 4.3–5.3 GHz observations of 20 “Arp 220-like” LIRGs. This frequency range contains a rich part of the spectrum of Arp 220, with transitions of HCN ($v_2 = 1$) at 4488 MHz, excited OH $2\Pi_{1/2}$, $J = 1/2$ at 4660, 4750, and 4765 MHz, H₂CO at 4829 MHz and CH₂NH at 5290 MHz. The aim was to determine

the occurrence rate of molecular spectra similar to Arp 220 among (U)LIRGS.

The sample of 20 galaxies were selected on the basis of having known $\lambda 18 \text{ cm}$ OH-megamasers (P. S. Chen et al. 2007), formaldehyde lines (E. Araya et al. 2004), compact starbursts (J. J. Condon et al. 1991) or far-IR emission lines similar to Arp 220 (L. Armus et al. 1990). The sample was also limited to $z < 0.033$ and $S_{6 \text{ cm}} > 20 \text{ mJy}$. NGC 660 was included on the basis of having both a formaldehyde absorption feature and a far-IR spectrum similar to Arp 220. However, it was not noted as having either $\lambda 18 \text{ cm}$ OH-megamaser emission or the extremely-high star-formation rate of Arp 220.

Two of the sample galaxies were found to possess almost identical spectra to Arp 220 (R. F. Minchin et al. 2009). However, the detailed line spectrum of NGC 660 did not resemble that of Arp 220. Nevertheless, it did yield the biggest surprise of the project in the form of excited-OH transitions at 4660, 4750, and 4765 MHz showing unprecedented transient behavior in intensity and line profiles such as had never been previously reported for these transitions in extragalactic objects. In addition, the variability of these OH spectral lines turned out to be closely mimicked over a 10 yr period by secular changes in the cm wavelength radio-continuum emission. Here, we present decade-long single-dish interferometric observations of this enigmatic event.

The observations we present in this paper demonstrate that the event causing the remarkable transient spectral-line and continuum emission seen by us in NGC 660 is occurring at the very center of this galaxy. Continuum variability of many extragalactic radio sources, and in particular blazars, quasars, and other compact radio sources, have been recognized through detailed monitoring of flux densities at centimetric and



Original content from this work may be used under the terms of the [Creative Commons Attribution 4.0 licence](#). Any further distribution of this work must maintain attribution to the author(s) and the title of the work, journal citation and DOI.

millimetric wavelenths, (e.g., M. F. Aller et al. 2017 and references therein). Such variability is found on all timescales from intraday to decades. T. Hovatta et al. (2008) studied a large sample of active galactic nuclei (AGNs) across the cm and mm wave window, identifying distinct transient flares in their flux density curves. They calculated that the duration for 150 flares at 37 GHz and 31 flares at 230 GHz varied from 0.3 to 13.2 yr, noting that the rise and decay times of the flares seem approximately equal, with the decay time typically being 1.3 times the rise time.

Also showing transient continuum radio emission, particularly from within the nuclear regions of LIRGs, are young supernovae (e.g., M. F. Bietenholz et al. 2021), and tidal disruption events (TDEs). The latter occur when a star passes within the tidal radius of the central supermassive black hole (SMBH) of a galaxy, disrupting the star and ejecting some 50% of its material, possibly in the form of jets. A recent review of the radio properties of TDEs was published by K. D. Alexander et al. (2020).

In this paper, we present the broad details of our NGC 660 observations and their results. Sections 2 and 3 detail the Arecibo, single-dish spectral-line-radio-continuum monitoring, and present the discovery of the NGC 660 “Outburst.” In Section 4, we discuss new VLA and High Sensitivity Array (HSA) very long baseline interferometry (VLBI) images, with the latter imaging both continuum and spectral-line data. These images help resolve the milliarcsecond structure of the central region of this galaxy. Phenomenological discussion regarding a plausible cause for the outburst follows in Section 5, and the conclusions are presented in Section 6.

The presentation of a full wide-frequency spectral-line survey of NGC 660, plus further spectral-line and continuum HSA high-resolution images, are deferred to a later paper. Detailed physical modeling of this source, including consideration of observations at wavelengths other than the radio, is also deferred to this future publication.

2. Arecibo Observations and Analysis

Over a year between 2007 December and 2008 December, NGC 660 and the 19 other “Arp 220-like” galaxies were observed with the 305 m radio telescope at Arecibo Observatory using the WAPP spectrometer in its dual-board mode, giving 8×100 MHz wide subbands. These were placed within a 1 GHz frequency range centered at 4.8 GHz to obtain coverage of a number of spectral lines of interest, including the excited-OH lines at 4660, 4750, and 4765 MHz. The observations were made in double position switching (DPS; T. Ghosh & C. J. Salter 2002) mode, with a continuum calibration (reference) source used to both remove standing waves from the spectrum and calibrate the flux-density scale. For NGC 660, the reference source selected was a nonvariable (compact steep spectrum) standard radio calibrator B0138+136 (3C 49). NGC 660 and 3C 49 are separated by only $0^\circ.5$ on the sky, and by only $0^\circ.25$ in decl.. Hence, we expect them to have possessed very similar telescope pointing errors, atmospheric opacities, and telescope spectral baseline ripples for all DPS observations. This will have resulted in very accurate relative flux-density calibration from epoch to epoch, which we estimate to be better than 5%. We believe that the flux densities that we derive for NGC 660 agree with the absolute scale of J. W. M. Baars et al. (1977) to better than 10%. The

data were analyzed using the standard Arecibo AOIDL package written by Phil Perillat.

After the discovery of transient emission in NGC 660 (see Section 3), follow-up observations were made in 2010 December and on three occasions in late 2011. Among the observations made on 2011 December 31 were a set that covered 1.1–10 GHz using the Arecibo *L*-, *S*-low, *C*-, *C*-high, and *X*-band receivers in order to obtain a detailed continuum spectrum for the galaxy at that epoch. A similar detailed continuum spectrum for NGC 660 was measured on 2014 August 14. From 2013, NGC 660 was monitored on a semiregular basis, both in respect of its *C*-band spectral lines, and its continuum flux density up until the end of 2018. However, the 2018 observations, taken after the Arecibo dish surface was damaged by Hurricane Maria, were of lower quality and are not included in the present analysis. The results presented here run up until 2017 August. In addition, a full, deep Arecibo spectral scan from 1.1 to 10 GHz was observed in 2012 November and December, results from which will be presented in a later publication.

3. Discovery of the Outburst in NGC 660

Spectra of NGC 660 from observing epochs in 2007 December and 2008 August showed little of interest apart from an already known H_2CO absorption line (e.g., E. Araya et al. 2004), and weak hydrogen recombination line emission. However, the spectrum taken in 2008 December revealed a significant detection of emission from the excited-OH main line at 4750 MHz and its satellite line at 4765 MHz. Follow-up observations in 2010 December not only confirmed the presence of this emission, but also showed that (a) the two emission lines had increased in intensity by almost a factor of four; (b) additional excited-OH line components, especially at higher velocity, had appeared for both of these transitions; and (c) counterparts of these components were also seen in the satellite line at 4660 MHz, mostly in absorption, but with a central feature in emission (Figure 1).

During the final third of 2011, all three transitions had become even stronger. Additionally, a further manifestation of unusual activity was discovered from the 2011 observations. When the *C*-band continuum flux densities for each of our epochs were computed, a steady increase over the 4 yr period from 2007 was seen. Figure 2 (left) shows the 4.7 GHz flux density of this “new continuum component” (NCC), derived by subtracting the preoutburst spectrum (using a best fit to all published pre-2008 flux density values), from our measurements. Figure 2 (right) displays the intensity changes of the excited-OH lines at a heliocentric velocity resolution of 10 km s^{-1} via the mean peak intensity of the strongest pair of emission components in the 4750 and 4765 MHz lines, and the mean of the peak absorption intensities for the two absorption components seen at 4660 MHz.

The radio continuum emission of NGC 660 between 1.25 and 8.7 GHz obtained on 2011 December 31, again after subtracting the preoutburst spectral fit to obtain the detailed spectrum of the NCC is shown in Figure 3 (top) with diamond symbols. This reveals a GHz-peaked spectrum (GPS) form, peaking close to 5 GHz and falling very rapidly toward lower frequencies. Figure 3 (bottom) presents the similarly derived spectrum for the NCC made from data acquired on 2014 August 14. This still shows a GPS form, although far less peaked than on the earlier occasion. For 2011 December 31, we

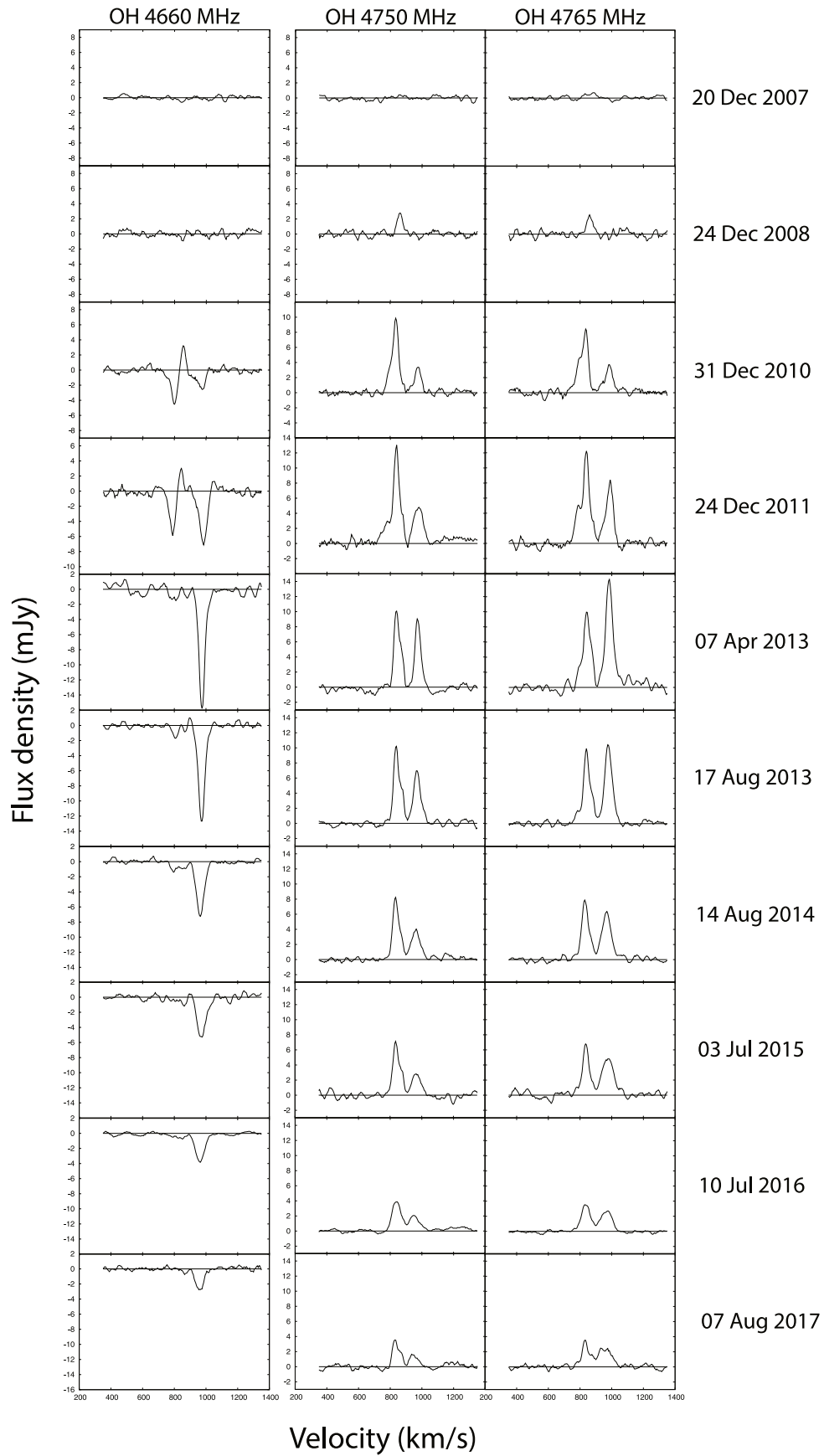


Figure 1. Sample excited-OH spectra of NGC 660 from late 2007 to 2017 August. The columns (left to right) show the 4660, 4750, and 4765 MHz lines, respectively, while time increases from top to bottom. Together, they display large secular changes in these molecular lines in NGC 660. The heliocentric velocity resolution is 10 km s^{-1} .

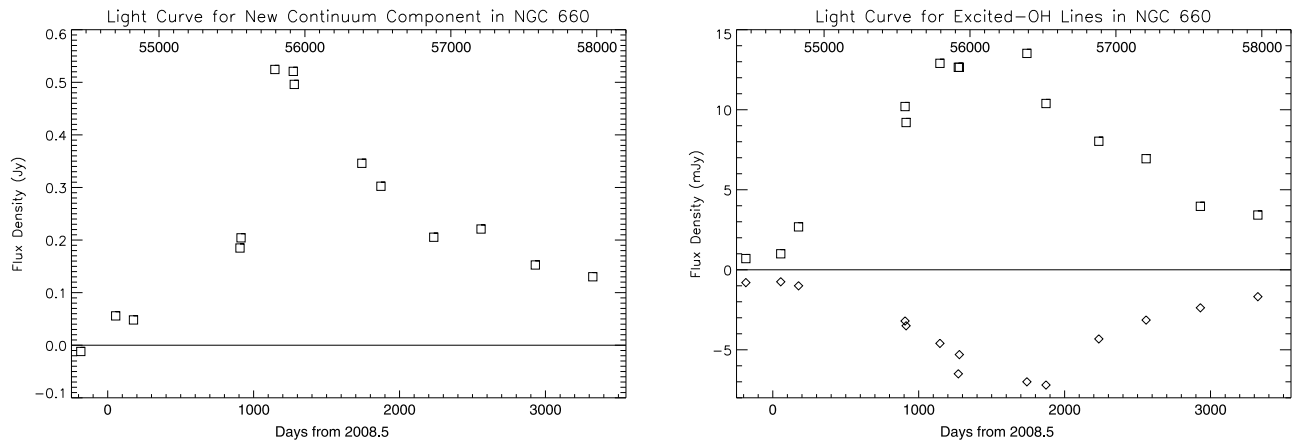


Figure 2. (Left) The 4.7 GHz continuum light curve of the NCC. (Right) The light curves of the excited-OH lines. Here, the data at the top (squares) represent the mean peak intensities of the strongest emission components at 4750 and 4765 MHz, while the symbols at the bottom (diamonds) show the mean peak intensity of the two 4660 MHz absorption components. The lower horizontal axis on both plots shows days from 2008.5, while the top axes show MJD.

derive a spectral index ($S \propto \nu^\alpha$) for the NCC at frequencies below its peak emission of $\alpha_{1.42}^{2.76} \sim +2.2$, consistent with total free-free or synchrotron self absorption. By 2014 August 14, this had changed to $\alpha_{1.40}^{2.76} \sim +0.4$. At this later date, the spectral index for frequencies above the emission peak of the NCC was $\alpha_{5.03}^{9.62} \sim -0.63$, characteristic of optically thin synchrotron emission. The NCC emission peak on 2011 December 31 was broadly situated at 5.5 ± 1.0 GHz, but had moved down to 4.0 ± 1.0 GHz by 2014 August 14. We note that such behavior is expected for a cloud of synchrotron-radiating relativistic particles that is initially opaque out to high radio frequencies, but which with expansion becomes optically thin at successively lower frequencies (H. van der Laan 1966).

While our preoutburst 4.8 GHz H_2CO absorption spectrum agrees well with published data, the postoutburst spectrum shows detailed differences. Subtracting the pre- and postoutburst spectra for this transition reveals three narrow absorption lines against the continuum emission of the NCC (Figure 4). In addition, in late 2011 December we obtained a small number of L -band spectra for NGC 660. For H I, a narrow absorption feature is clearly seen at the velocity of the deepest new H_2CO absorption line seen in Figure 4. The OH main lines at 1665 and 1667 MHz show somewhat different detailed profiles to those previously published by E. Araya et al. (2004). Much more remarkably, the 1612 and 1720 MHz satellite OH lines are not only stronger than the main lines (up to 27 mJy) and show multiple components, but are closely conjugate (i.e., emission at 1612 MHz shows absorption of identical line profile at 1720 MHz, and vice versa). The physical explanation for their “conjugate” nature depends upon how the two higher (hyperfine) energy levels of the OH molecule’s ground state, i.e., $^2\Pi_{3/2} + F = 2$, and $F = 1$ are populated. The two possible pathways are intraladder $^2\Pi_{5/2} \rightarrow ^2\Pi_{3/2}$ at $119 \mu\text{m}$ and the cross ladder $^2\Pi_{1/2} \rightarrow ^2\Pi_{3/2}$ at $79 \mu\text{m}$. Excited-OH molecules will cascade down to the ground level via either of these two transitions. With the applications of the selection rules (that parity has to change and $|\Delta F| = 1$ or 0), the intraladder cascade would then cause overpopulation of the $F = 2$ level, resulting in the 1720 MHz line being observed in emission and the 1612 MHz line in absorption. In the case of cross-ladder pumping, the situation will be reversed with the $F = 1$ level being overpopulated leading to the 1612 MHz line appearing in emission and 1720 MHz line in absorption. Which route is

more relevant depends upon the details of the pumping (M. Elitzur 1992). More details concerning the physical process leading to conjugate satellite transitions are discussed by H. J. van Langevelde et al. (1995) and in references therein. Examples of such lines in Galactic interstellar clouds can be found in W. M. Goss (1968) and J. L. Caswell & R. F. Haynes (1975), and for extragalactic sources such as Cen A (H. J. van Langevelde et al. 1995) and PKS 1413+135 (N. Kanekar et al. 2004).

The presence of such effects can be used to determine constraints on the OH-column density in the emitting/absorbing region. We cannot say whether these conjugate satellite OH lines have appeared since the occurrence of the outburst; certainly their velocities differ from those of both the new excited-OH components, and the H_2CO absorption lines seen against the NCC. The full spectral-line data for the source as a function of observing epoch will be presented in a future publication.

Preliminary results from the observations were presented by R. F. Minchin et al. (2013). Following that announcement, observations made with e-MERLIN and the European VLBI Network by M. K. Argo et al. (2015) confirmed that the outburst was a nuclear event. However, these lacked the spatial and spectral resolution of our HSA observations, and the time series of our Arecibo observations, while concluding that the outburst was likely to be the onset of a new period of AGN activity.

4. Interferometric Follow-up

Two scenarios that could be employed as explanations for the outburst in NGC 660 are:

1. First, that this represents a heavily obscured supernova (SN) outburst occurring in 2007–2008. Adopting the Tully–Fisher z -independent distance for NGC 660 of 14.7 ± 2.2 Mpc (C. M. Springob et al. 2009) gives a 5 GHz continuum luminosity for the NCC of $1.3 \pm 0.2 \times 10^{22} \text{ W Hz}^{-1}$. However, M. F. Bietenholz et al. (2021) use their 2–10 GHz sample of 294 core-collapse SNe to derive a median spectral luminosity at peak of $10^{18.5 \pm 1.6} \text{ W Hz}^{-1}$, with SNe of class II n reaching peak luminosities of $10^{19.5 \pm 1.1} \text{ W Hz}^{-1}$. The NCC would thus represent an unusually luminous core-collapse radio SN.

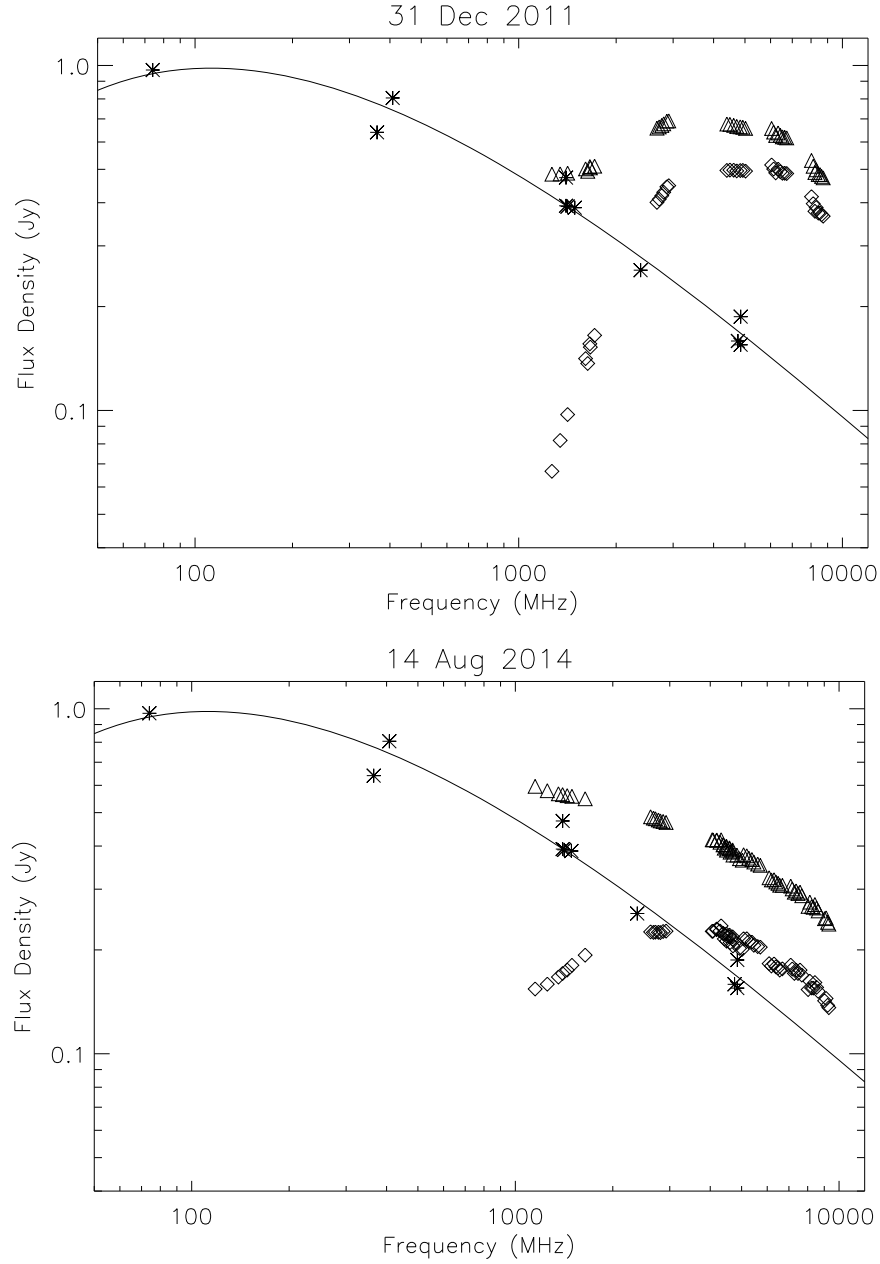


Figure 3. The radio continuum spectrum of NGC 660 on 2011 December 31, near the epoch of the peak of the outburst (top), and on 2014 August 14 (bottom). Stars denote preoutburst flux densities from the literature, with the solid line showing a spectral fit to this data. Triangles mark total measured flux densities, while diamonds show these total values minus the preoutburst spectral fit, i.e., the spectrum of the transient NCC alone.

To date, only a single radio detection has been made of a Type-1a SN (E. C. Kool et al. 2023; X. Yang et al. 2023). This was classified by E. C. Kool et al. (2023) as being of Type 1a-CSM, developing an atypical Type 1a optical spectrum as it evolved. Both E. C. Kool et al. (2023) and X. Yang et al. (2023) find a 5.1 GHz continuum luminosity of $\sim 1.5 \times 10^{20} \text{ W Hz}^{-1}$. Were the NCC to be a supernova remnant that had been expanding freely at the canonical value of 10^4 km s^{-1} , (see A. Pedlar et al. 1999 who measured an expansion velocity of $9850 \pm 1500 \text{ km s}^{-1}$ for a young SN in the starburst galaxy M82), for 1000 days, it would then have presented a diameter of $\sim 1 \text{ mas}$ and would have been expected to show a ring or disk structure. However, this would have been barely resolved by terrestrial VLBI at cm

wavelengths such as we present in Section 4.2 and would have appeared as a quasicompact source containing essentially the total flux density of the NCC. We detect no such component in our VLBI images of Section 4.2.

2. The second possible explanation is that we are seeing the result of an outburst originating at the very center of NGC 660 that commenced 3–4 yr before the 2011/2012 epoch. For this, a core-jet appearance would be expected, with an expansion velocity higher than for the SN case. With the light curves of the NCC and the OH features being so similar, the gas involved in the molecular-line emission must be no more than a light month or so separated from the location of the continuum emission. Hence, the OH emission would be expected to be distributed over a broadly similar area to the continuum feature.

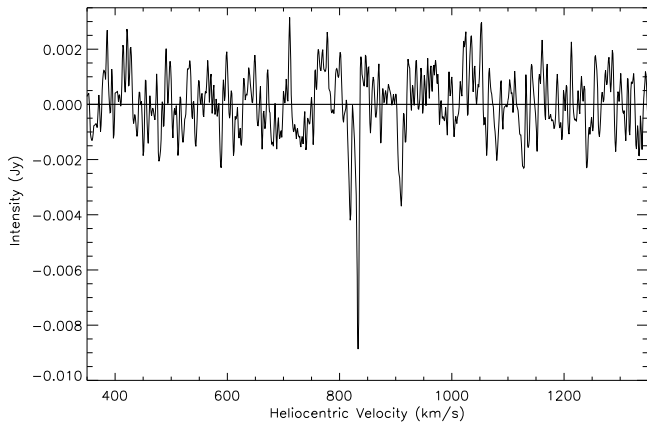


Figure 4. The spectrum of H_2CO against the NCC. This was obtained by subtracting the line spectrum of 2007 December (i.e., preoutburst) from the spectrum of 2011 December, and shows new sharp absorption features.

4.1. The VLA Observations

Given these scenarios, we decided to use VLBI imaging to help determine what was actually happening within NGC 660. To obtain a subarcsecond position for the NCC, such as was necessary for the high-resolution VLBI follow-up, we were first granted observing time with the VLA of the NRAO, Socorro, New Mexico.

The VLA observations were carried out in a single 1.5 hr session on 2012 May 6 in the DnC configuration. Two 1 GHz wide bandwidths were observed simultaneously, centered at 8.5 and 11.5 GHz. The WIDAR correlator was configured to deliver 8×128 MHz subbands in each 1 GHz window for all four polarization products (RR, LL, RL, LR). Each 128 MHz subband was further subdivided into 64 spectral channels. The standard source 3C48 was used to calibrate the absolute flux density scale, with the source J0121+1149 being used as the complex gain calibrator. The total on-source time was about 55 minutes. At the time of the observations, 10 of the antennas were still equipped with the legacy X-band receivers, which were sensitive only in the 8–8.8 GHz frequency range, while the remaining antennas were equipped with the new wide-band X-band receivers that cover the frequency range 8–12 GHz. Thus, the data for 8–8.8 GHz were from all the antennas that participated in the observations, while the data for 8.8–9 GHz and 11–12 GHz were only from the antennas that had the new receivers.

Editing, calibration, imaging, and deconvolution of the data were performed using the Astronomical Image Processing System of the NRAO (E. W. Greisen 2003). After applying the phase and amplitude gain corrections from J0121+1149 to the NGC 660 data, the target data were split into two files corresponding to the 2×1 GHz frequency windows, and averaged in frequency. Both phase and amplitude self calibration, plus imaging, were performed in an iterative cycle for each separate 1 GHz window to further improve the image quality.

Figure 5 shows the final continuum images NGC 660 at 8.5 and 11.5 GHz. The rms noises in these images are 75 and $105 \mu\text{Jy beam}^{-1}$, with restoring beams of $2''.59 \times 2''.06$ (P.A. = 43°) and $3''.00 \times 2''.08$ (P.A. = 22°), respectively. A two-dimensional Gaussian function was fitted on the continuum source in each image. The best-fit positions of the source are $\alpha = 01^{\text{h}}43^{\text{m}}02^{\text{s}}.320$, $\delta = 13^\circ38'44''.96$, and $\alpha = 01^{\text{h}}43^{\text{m}}02^{\text{s}}.319$, $\delta = 13^\circ38'44''.97$ in the 8.5 and 11.5 GHz images, respectively.

These positions agree to better than $0''.1$ with that measured for the preoutburst radio core at 8.4 GHz from VLA A-array data by M. E. Filho et al. (2002). As the majority of the flux density in our images will have originated from the NCC, this confirms its location at the core of NGC 660.

At 8.5 GHz, the peak and total flux densities were $385.8 \pm 0.1 \text{ mJy beam}^{-1}$ and $414.0 \pm 0.2 \text{ mJy}$, respectively. The source was resolved at this frequency, with a nominal deconvolved size of $0''.89 \times 0''.35$ (P.A. = 49°). At 11.5 GHz, the peak and total flux densities were $309.1 \pm 0.1 \text{ mJy beam}^{-1}$ and $333.6 \pm 0.2 \text{ mJy}$, respectively. The source was resolved at this frequency, with a nominal deconvolved size of $0''.96 \times 0''.42$ (P.A. = 48°).

4.2. The HSA (VLBI) Observations

In 2012 July, HSA VLBI observations at the C and X bands were made to image the NCC continuum structure with ~ 1 mas resolution, and to investigate the excited-OH emission/absorption and H_2CO absorption against the NCC. These observations used the HSA with stations from the Very Long Baseline Array (VLBA), along with the 100 m Effelsberg radio telescope, the 305 m Arecibo telescope and the 100 m Green Bank Telescope. For the C-band observations, the Saint Croix and Los Alamos VLBA stations were not available, giving a total of 11 antennas in the array. For the X-band observations all ten VLBA stations participated.

Analysis of the C- and X-band data has produced remarkable continuum images, (Figure 6). The milliarcsec structure shows a triple source consisting of a flat-spectrum ($\alpha \sim 0.0$) compact central component, with a pair of more diffuse steep-spectrum features disposed roughly E-W on either side. The western feature consists of a bright pair of “hot spots,” with no jet emission being seen. In contrast, the eastern feature has the form of an edge-brightened jet, with the center lines of the edge-brightened features pointing through the central source, toward the opposing western hot spots. The overall emission distribution seems to be consistent with the canonical structure of a classical radio source (J. J. Condon & S. M. Ransom 2016), perhaps in this case with a pair of rapidly precessing, relativistic jets emanating from the active nucleus, with the jet directions precessing along the surfaces of diametrically opposed cones. The jet to the east would be the approaching Doppler-boosted jet, with emission from lines of sight passing through the edges of that cone being further enhanced by the greater geometrical, line-of-sight depths encountered there. In contrast, the receding jet to the west would be Doppler diminished and hence not seen. However, this western jet would be responsible for the western hot spots where it interacts with the circumnuclear medium.

As we present only single-epoch VLBI observations in Figure 6, it may be asked whether the core, jet, and hotspot emission revealed there might not preexist the present outburst? However, two pieces of evidence suggest this not to be the case. First, M. E. Filho et al. (2004) observed the core of NGC 660 with the VLBA at C band in 2001 September, setting a 5σ upper limit to the peak flux of $0.5 \text{ mJy beam}^{-1}$, and not making any detection. Their observations should have easily detected (with SNR > 70) the hot spots seen on both sides of the core were these to have been present at that time. Second, linear interpolation between the two nearest Arecibo single-dish 4.7 GHz continuum flux density estimates for the NCC yields a value of 447 mJy for 2013 mid July. The total flux density

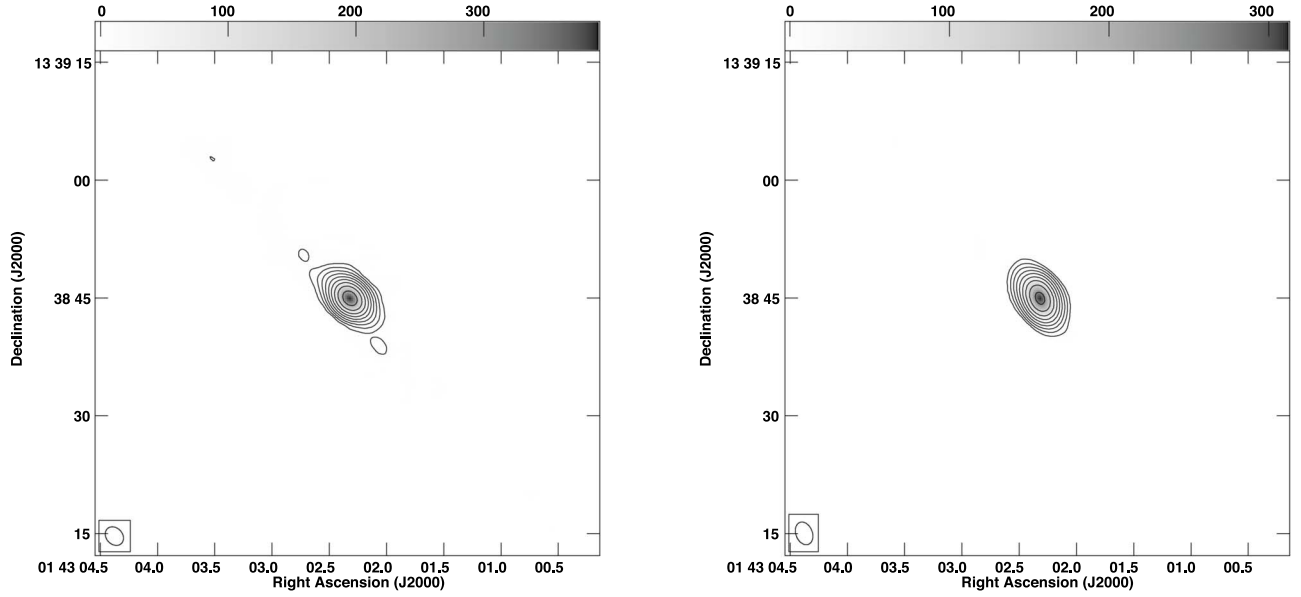


Figure 5. Continuum images of NGC 660 at 8.5 GHz (left) and 11.5 GHz (right). For the 8.5 GHz image, the rms noise level is $75 \mu\text{Jy beam}^{-1}$ and the restoring beam size is $2''.59 \times 2''.06$ (P.A. = 43°). For the 11.5 GHz image, the rms noise level is $105 \mu\text{Jy beam}^{-1}$ and the restoring beam size is $3''.00 \times 2''.08$ (P.A. = 22°). The contour levels are at $-1, 1, 2, 4, \dots, 256 \text{ mJy beam}^{-1}$. The gray-scale range is indicated at the top of each image in units of mJy beam^{-1} .

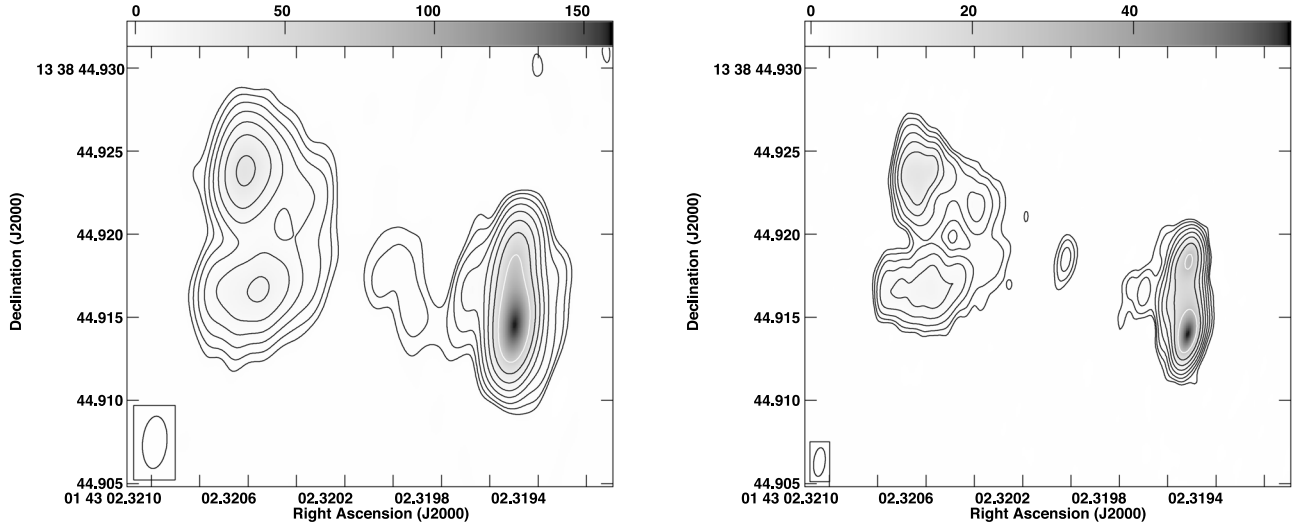


Figure 6. (Left) The HSA continuum images of NGC 660 at 4.7 GHz, HPBW = $3.1 \times 1.5 \text{ mas}$ at P.A. = -4° , and (right) at 8.4 GHz, HPBW = $1.6 \times 0.7 \text{ mas}$ at P.A. = -5° . Contour levels are at $2.5\sigma \times 2.5, 5, 10, 20, 40, 80, 160, 320$ with $\sigma = 80 \mu\text{Jy}$ at 4.7 GHz and $\sigma = 36 \mu\text{Jy}$ at 8.4 GHz. The gray-scale range is indicated at the top of each image in units of mJy beam^{-1} .

integrated from our 4.7 GHz VLBI image of Figure 6 (left) at that epoch is 458 mJy. The outstanding agreement of these two values indicates the identity of the Arecibo NCC and the VLBI structure revealed by our HSA observations.

The 2012 July C-band VLBI observations showed that the excited-OH and H_2CO lines found at Arecibo were coincident with the continuum hot spots of the NCC revealed by the HSA observations, confirming at least near physical coincidence between these continuum features and the spectral outburst in NGC660 (Figure 7). The velocity structure of the OH lines from the C-band data cubes shows that those associated with the eastern hot spots lie at considerably lower radial velocities than those associated with the region of the northwestern hotspot. This is consistent with the above suggestion that the eastern VLBI components represent the approaching jet, with the western VLBI hot spots defining the receding jet. A full

analysis of the spectral properties will be presented in a later paper.

Assuming the central compact component seen at X-band to be the galaxy's active nucleus, the angular distances between it and the peaks in the four "hot spots," as measured from the 8.4 GHz image of Figure 6, are:

1. NE hotspot \leftrightarrow central source = 10.2 mas (11.4 mas to the outer edge);
2. SE hotspot \leftrightarrow central source = 10.5 mas (11.6 mas);
3. NW hotspot \leftrightarrow central source = 7.4 mas (8.4 mas);
4. SW hotspot \leftrightarrow central source = 8.4 mas (9.1 mas).

The opening angles from the central component to the two hot spots on either side are $\approx 34^\circ$ to the eastern hotspot pair, and $\approx 23^\circ$ to the western pair.

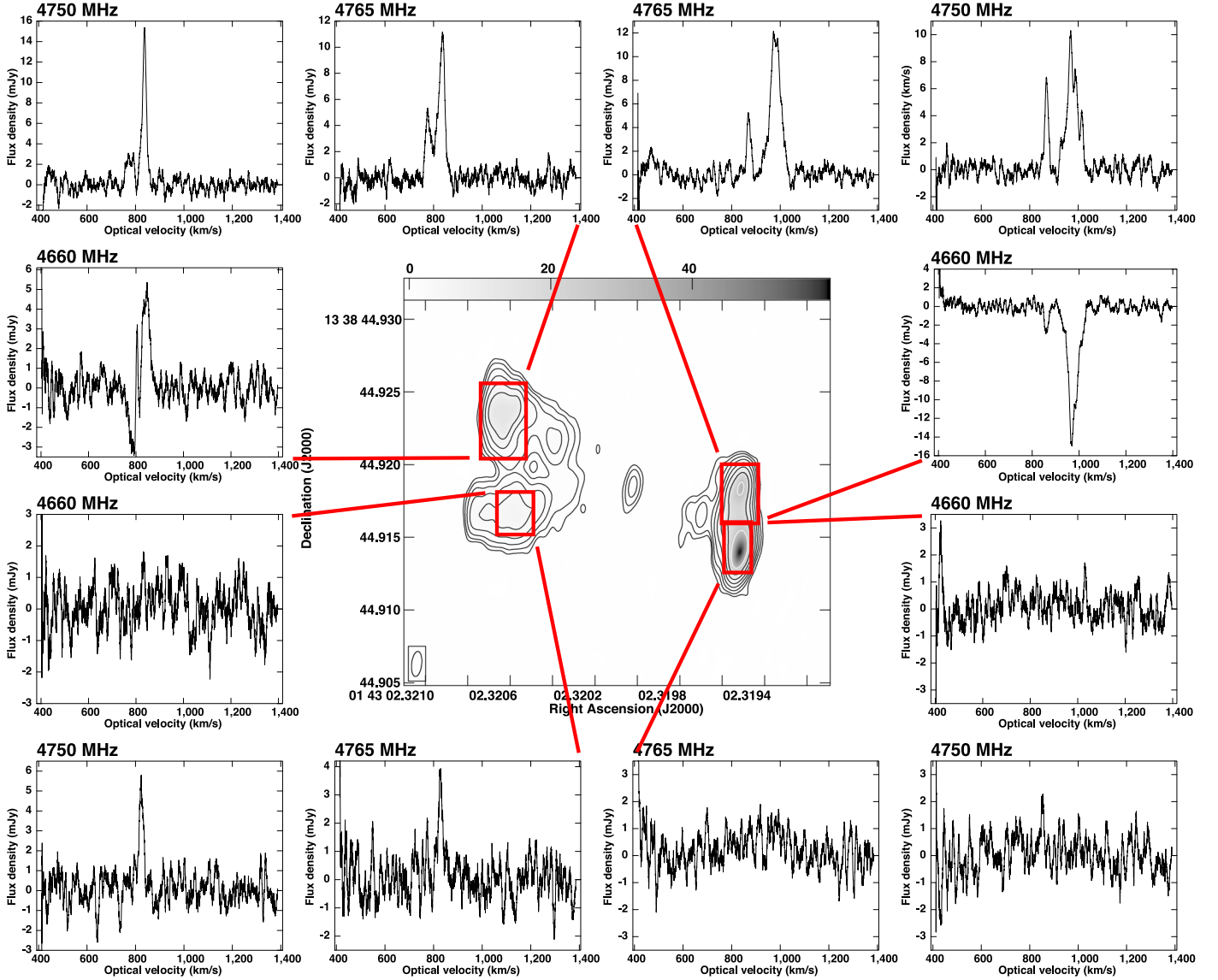


Figure 7. The integrated excited-OH lines from the regions of the four “hot spots” seen in the X-band image of Figure 6. The higher velocity components occur exclusively against the northwestern hotspot, while those at lower velocities are mainly found against the two eastern hot spots.

4.3. Implications of the VLBI Results

If the NCC is an intrinsically symmetric double radio source, in which the outer components advance from the nucleus at a velocity of $v = \beta c$ along an axis inclined at an angle ϕ to the line of sight, then (D. J. Saikia 1981)

$$\theta_1/\theta_2 = (1 + \beta \cos \phi)/(1 - \beta \cos \phi) \quad (1)$$

where θ_1 and θ_2 are the apparent separations of the approaching and receding components from the radio core. For the above displacements from the central source (assumed to be the active nucleus), we have a ratio of $10.2/8.4 = 1.214$ for the NE/SW hotspot pair and a ratio of $10.5/7.4 = 1.419$ for the NW/SE hotspot pair. These give $\beta \cos \phi = 0.097$ for the first pair and $\beta \cos \phi = 0.173$ for the second pair. Combining these gives a value of: $\beta \cos \phi = 0.135 \pm 0.038$.

In addition, for the Tully–Fisher distance of 13.6 Mpc, the projected distance from the core to the approaching hot spots is 0.68 ± 0.01 pc. If the approaching jet was launched from close to the core, and had been flowing out for T yr at the epoch of

the HSA observations, then its apparent velocity in the plane of the sky would be $6.65 \pm 0.10 \times 10^5/T \text{ km s}^{-1}$, giving $1.6 \pm 0.2 \times 10^5 \text{ km s}^{-1}$ for $T = 4.1 \pm 0.5$ yr (assuming an epoch of 2008.5 ± 0.5 , i.e., midway between the 2007 December and 2008 December observations, for the outburst date; see Figure 1). This gives the apparent perpendicular velocity as a fraction of the speed of light, $\beta_{\perp} = 0.53 \pm 0.07$.

For a component moving at an angle ϕ to the line of sight (J. J. Condon & S. M. Ransom 2016), β_{\perp} is given by:

$$\beta_{\perp} = \beta \sin \phi / (1 - \beta \cos \phi). \quad (2)$$

Substituting $\beta \cos \phi = 0.135 \pm 0.038$ and $\beta_{\perp} = 0.53 \pm 0.07$ into this equation yields $\beta \sin \phi = 0.46 \pm 0.14$.

The above values of $\beta \cos \phi$ and $\beta \sin \phi$ yield $\tan \phi = 3.4 \pm 1.2$ and thus $\phi = 74^{+4}_{-8}$ degrees and $\beta = 0.48 \pm 0.16$. Of course, how much faith can be placed on these values is dependent on many assumptions: were the jets launched from the proximity of the galaxy nucleus, and when? Are the opposing jets colinear? Is the ambient medium symmetric on opposite sides of the nucleus? However, it is suggestive that the

new continuum component is mildly relativistic, and moving closer to the plane of the sky than to the line of sight.

The mean brightness of the jet toward the east is at least 4 times greater than the jet toward the west, possibly much more. It is of interest (K. I. Kellermann & F. N. Owen 1988) that a jet with a positive velocity component toward the observer is Doppler boosted by a factor of $[\gamma^{(\alpha-3)}(1 - \beta\cos(\phi))]^{(\alpha-3)}$, where $\gamma = (1 - \beta^2)^{-0.5}$ and α is the spectral index of the jet. The jet pointing away from the observer will be diminished by a similar factor. The value of α for the NCC between 7.1 and 9.6 GHz at that epoch was $\alpha \sim -0.9$ from our Arecibo monitoring of the source flux density. For $\phi \approx 74^\circ$ and $\beta \approx 0.48$, the brightness ratio of the opposing jet features would be ≈ 25 .

5. Discussion

Given the consistency of the HSA continuum images with an outburst at the nucleus of NGC 660, the existence of mildly relativistic jets, and the lack of a single quasicompact component containing the majority of the NCC flux density, the hypothesis that the NGC 660 outburst represents a heavily obscured supernova explosion now seems untenable. Indeed, we appear to be seeing an outburst in the nucleus of NGC 660 that commenced in the radio in 2008. The morphology revealed by our VLBI observations is consistent with a rapidly precessing, diametrically opposed pair of radio jets from the core of the galaxy. However, the question remains as to what caused these jets? Plausible explanations for the NGC 660 outburst might be that the observed VLBI jets have been launched by either (a) the infall of a gas cloud on to the central SMBH, or (b) a TDE caused by a star passing within the “tidal radius” of the SMBH and being torn asunder, with part of its material being ingested by the BH, and the rest being ejected as a high velocity jet (M. J. Rees 1988; B. A. Zauderer et al. 2011; G. C. Bower et al. 2013). If this were a TDE, then the evolution of the source morphology and the detailed line and continuum radio light curves would provide detailed tests for many of the models proposed for these objects.

The possibility of the disruption of a very massive star is non-negligible given the presence of a nuclear starburst in this galaxy. In addition, the presence of a massive polar ring around the main galaxy disk indicates a collision with a massive companion within the past few billion years (W. van Driel et al. 1995). Indeed, van Driel et al. note that the shape of NGC 660’s inner bulge may indicate peculiar stellar orbits in the bulge, possibly making TDEs not unlikely events in this galaxy.

The major challenge for explaining the NGC 660 outburst as a TDE is that most such events, at all wavelength ranges, have evolved on timescales of less than one year (K. D. Alexander et al. 2020) and have light curves with a rapid initial rise followed by a slow decline. Most TDEs have also been found in quiescent, poststarburst galaxies (K. D. French et al. 2017). In contrast, the NGC 660 outburst occurred in a star-forming LIRG, peaked three years after initial detection (four years after the previous nondetection) and was followed by us for almost a decade. While a likely TDE lasting for over a decade was discovered in the soft X-ray range within a dwarf starburst galaxy by D. Lin et al. (2017), which the authors suggest represented the disruption of a very massive star, this event had a fast rise time in luminosity (<4 months), and then underwent a very slow decay that was followed for over 10 yr, very different in shape to the light curve seen in NGC 660 (Figure 2). There have also been observations of late radio emission from TDEs (e.g., A. Horesh et al. 2021a, 2021b;

Y. Cendes et al. 2022), with continuum peaks as late after optical detection as the time from first (radio) detection to the peak in NGC 660. However, in these cases there was no detectable radio emission until close to the time of the radio peak, followed by a steep rise ascribed to the late launching of a jet. This scenario does not fit with what has been seen in NGC 660. Further, as noted by M. K. Argo et al. (2015), archival X-ray data show no sign of a peak in X-ray luminosity as would be expected if this were a TDE.

The shape of the light curve for this event points toward it being the accretion of a gas cloud rather than a TDE. This does not seem to be the dawn of a new period of sustained AGN activity, as suggested by M. K. Argo et al. (2015), as the continuum light curve peaked in late 2011 and fell back to below 25% of that peak by 2017, while the OH emission and absorption peaked by the end of 2012 and have also fallen back to below 25% of those peaks. Rather, it seems likely that this outburst was a single, extended event—most likely the ingestion of a gas cloud over a prolonged period.

6. Conclusion




We serendipitously detected a quasismultaneous continuum and spectral-line outburst in NGC 660 during a line survey with the 305 m Arecibo radio telescope. Over a decade, we have monitored both the continuum outburst, and the variable emission and absorption spectra of the excited-OH molecule at the C band. High-resolution VLBI follow-up has revealed these remarkable transient features to be located at the center of the galaxy and to have a morphology consistent with a rapidly precessing, two-sided jet. Analysis of the approaching and receding components of the jet suggests that it is closer to the plane of the sky than to the line of sight and that it is mildly relativistic. The source of the outburst is likely to be the accretion of either a gas cloud or debris from a TDE onto the central SMBH. From the shape of the light curve, accretion of a gas cloud would appear the more likely of these two possibilities.

Acknowledgments

We thank an anonymous referee for a number of useful suggestions which have considerably improved the paper. Arecibo Observatory was operated by Cornell University until 2011 under a cooperative agreement with the National Science Foundation (NSF). From 2011 until 2018 by SRI International under a similar cooperative agreement, in alliance with Ana G. Méndez-UMet and USRA. From 2018 April until 2023 August it was operated by the University of Central Florida under a cooperative agreement with the NSF and in alliance with Universidad Ana G. Méndez and Yang Enterprises, Inc.

The National Radio Astronomy Observatory (NRAO) is a facility of the NSF operated under cooperative agreement by Associated Universities, Inc.

ORCID iDs

R. F. Minchin  <https://orcid.org/0000-0002-1261-6641>
E. Momjian  <https://orcid.org/0000-0003-3168-5922>
B. Catinella  <https://orcid.org/0000-0002-7625-562X>

References

- Alexander, K. D., van Velzen, S., Horesh, A., et al. 2020, *SSRv*, 216, 81
- Aller, M. F., Aller, H. D., & Hughes, P. A. 2017, *Galax*, 5, 75
- Araya, E., Baan, W. A., & Hofner, P. 2004, *ApJS*, 154, 541

- Argo, M. K., van Bemmell, I. M., Connolly, S. D., et al. 2015, *MNRAS*, **452**, 1081
- Armus, L., Heckman, T. M., & Miley, G. K. 1990, *ApJ*, **364**, 471
- Baars, J. W. M., Genzel, R., Pauliny-Toth, I. I. K., et al. 1977, *A&A*, **61**, 99
- Bietenholz, M. F., Bartel, N., Argo, M., et al. 2021, *ApJ*, **908**, 75
- Bower, G. C., Metzger, B. D., Cenko, S. B., et al. 2013, *ApJ*, **763**, 84
- Caswell, J. L., & Haynes, R. F. 1975, *MNRAS*, **173**, 649
- Cendes, Y., Berger, E., Alexander, K. D., et al. 2022, *ApJ*, **938**, 28
- Chen, P. S., Shan, H. G., & Gao, Y. F. 2007, *AJ*, **133**, 496
- Condon, J. J., Huang, Z.-P., Yin, Q. F., & Thuan, T. X. 1991, *ApJ*, **378**, 65
- Condon, J. J., & Ransom, S. M. 2016, *Synchrotron Radiation, Essential Radio Astronomy* (Princeton, NJ: Princeton Univ. Press), 196
- Elitzur, M. 1992, *Astronomical Masers, Astrophysics and Space Science Library* (Dordrecht: Kluwer)
- Filho, M. E., Barthel, P. D., & Ho, L. C. 2002, *ApJS*, **142**, 223
- Filho, M. E., Fraternali, F., Markoff, S., et al. 2004, *A&A*, **418**, 429
- French, K. D., Arcavi, I., & Zabludoff, A. 2017, *ApJ*, **835**, 176
- Ghosh, T., & Salter, C. J. 2002, in *ASP Conf. Proc. 278, Single-Dish Radio Astronomy: Techniques and Applications*, ed. S. Stanimirovic et al. (San Francisco, CA: ASP), 521
- Goss, W. M. 1968, *ApJS*, **15**, 131
- Greisen, E. W. 2003, *Information Handling in Astronomy—Historical Vistas*, Vol. 285 (Dordrecht: Kluwer), 109
- Horesh, A., Cenko, S. B., & Arcavi, I. 2021a, *NatAs*, **5**, 491
- Horesh, A., Sfaradi, I., Fender, R., et al. 2021b, *ApJL*, **920**, L5
- Hovatta, T., Nieppola, E., Tornikoski, M., et al. 2008, *A&A*, **485**, 51
- Kanekar, N., Chengalur, J. N., & Ghosh, T. 2004, *PhRvL*, **93**, 051302
- Kellermann, K. I., & Owen, F. N. 1988, *Galactic and Extragalactic Radio Astronomy* (New York: Springer-Verlag), 563
- Kool, E. C., Johansson, J., Sollerman, J., et al. 2023, *Natur*, **617**, 477
- Lin, D., Guillochon, J., Komossa, S., et al. 2017, *NatAs*, **1**, 33
- Minchin, R. F., Catinella, B., Ghosh, T., et al. 2009, *BAAS*, **41**, 328
- Minchin, R. F., Ghosh, T., Momjian, E., et al. 2013, *AAS Meeting Abstracts*, **221**, 157.06
- Pedlar, A., Muxlow, T. W. B., Garrett, M. A., et al. 1999, *NewAR*, **43**, 535
- Rees, M. J. 1988, *Natur*, **333**, 523
- Saikia, D. J. 1981, *MNRAS*, **197**, 11P
- Salter, C. J., Ghosh, T., Catinella, B., et al. 2008, *AJ*, **136**, 389
- Springob, C. M., Masters, K. L., Haynes, M. P., et al. 2009, *ApJS*, **182**, 474
- van der Laan, H. 1966, *Natur*, **211**, 1131
- van Driel, W., Combes, F., Casoli, F., et al. 1995, *AJ*, **109**, 942
- van Langevelde, H. J., van Dishoeck, E. F., Sevenster, M. N., et al. 1995, *ApJL*, **448**, L123
- Yang, X., Liu, Z., Shan, H., et al. 2023, *ATel*, **16080**
- Zauderer, B. A., Berger, E., Soderberg, A. M., et al. 2011, *Natur*, **476**, 425